Bulgarian Chemical Communications, Volume 45, Special Issue B (pp. 11-17) 2013

Effect of the sublayer thickness and furnace annealing on the crystallographic structure and grain size of nanocrystalline $Zn_xCd_{1-x}Se$ thin films

D.D. Nesheva[1*], I.E. Bineva[1], M. Danila[2], A. Dinescu[2], Z.M. Levi[1], Z.I. Aneva[1], R. Muller[2]

[1]*Institute of Solid State Physics, Bulgarian Academy of Sciences, 72 Tzarigradsko chaussee blvd., 1784 Sofia, Bulgaria*
[2]*National Institute for R&D in Microtechnologies – IMT Bucharest 126A, Erou Iancu Nicolae Street, 077190 Bucharest, Romania*

Received October 17, 2013; Revised November 25, 2013

X-ray diffraction (XRD) and high resolution scanning electron microscopy (HRSEM) were used to study the influence of the sublayer thickness and furnace annealing on the crystallographic structure and microstructure of 400 nm thick films from $Zn_xCd_{1-x}Se$ with x = 0.4, 0.6 and 0.8. The films were prepared by consecutive deposition of ultrathin, island type sublayers of ZnSe and CdSe with various nominal thicknesses (0.08, 0.12 and 0.23 nm). Based on the X-ray diffraction results it has been concluded that independently of the sublayer thickness all films have predominantly cubic structure. Existence of a small amount of wurtzite phase has also been ascertained and the wurtzite phase decreases with increasing Zn content. The SEM images have revealed that in as-deposited films of each composition the thinner the sublayer thickness, the smaller the grain size. It has been also found that the internal strain in the annealed films with x=0.6 and 0.8 is higher than that in the as-deposited ones.

Keywords: thermal evaporation, $Zn_xCd_{1-x}Se$, annealing, X-ray diffraction, scanning electron microscopy, film structure

INTRODUCTION

Group II-VI compound semiconductors are important in a wide spectrum of applications. In particular, ternary compounds including zinc cadmium selenide ($Zn_xCd_{1-x}Se$) have attracted significant attention in the field of solar cells due to their band gap [1, 2] and lattice constant modulation by composition. Ternary II-VI semiconductors alloys (ZnCdSe, ZnSSe) included in ZnSe based quantum structures have also demonstrated considerable promise as short-wavelength light sources, fast switching devices, etc. [3-5].

Different methods have been used for deposition of $Zn_xCd_{1-x}Se$ films including vacuum techniques [6, 7], chemical vapour [8] and chemical bath [9] deposition, electrodeposition [1, 2]. The crystalllographic structure of $Zn_xCd_{1-x}Se$ films is rather sensitive to the preparation conditions. Both cubic [9, 10] or wurtzite [1] structure for all compositions in the range $0 \leq x \leq 1$, as well as transition from wurtzite in Cd-rich, to cubic in Zn-rich films, with a mixture of the two phases in between have been reported [11, 12]. Therefore for each preparation method the effect of the preparation conditions on the crystallographic structure of $Zn_xCd_{1-x}Se$ films has to be studied carefully.

Recently we have reported on preparation of nanocrystalline $Zn_xCd_{1-x}Se$ thin films by thermal evaporation in vacuum [13-15]. The film were produced by thermal evaporation of ZnSe and CdSe in vacuum and alloying of a large number of consecutively deposited island type sublayers of ZnSe and CdSe whose nominal thickness (i.e. the thickness of a film if continuous) is 0.12, 0.25 and 0.37 nm. The nominal thickness and film composition were defined by the deposition rates of both materials. Thus $Zn_xCd_{1-x}Se$ films with five different, well reproducible compositions were produced. Atomic force microscopy (AFM) phase images revealed a nanosized second phase on the surface of as-deposited films. The largest amount of the second phase was observed in the films with greatest nominal thickness of both sublayers and it disappeared after annealing at 673 K [15] while in the films with lowest nominal sublayer thickness no second phase was observed after furnace annealing at 473 K. The second phase on the film surface was related [14] to existence of nanosized Cd-enriched regions which may appear in the alloying process.

In this article we report production of $Zn_xCd_{1-x}Se$ films with three different compositions

* To whom all correspondence should be sent:
E-mail: nesheva@issp.bas.bg

© 2013 Bulgarian Academy of Sciences, Union of Chemists in Bulgaria

by applying the above described preparation technique but reducing considerably the nominal sublayer thickness. The effect of the sublayer thickness reduction on the film crystal structure and microstructure is explored by comparing the X-ray diffraction data of films prepared at different deposition rates. The influence of the film furnace annealing at 673 K on the crystal structure is also investigated.

EXPERIMENTAL

Thin films of $Zn_xCd_{1-x}Se$ with x = 0.4, 0.6 and 0.8 (x represents the Zn content, x = Zn/(Zn+Cd)) and thickness of 400 nm were prepared by simultaneous thermal evaporation of ZnSe and CdSe powders (Merck, Suprapure) from two independent tantalum crucibles. The films were deposited on Corning 7059 glass substrates (for the XRD measurements) and crystalline silicon (c-Si) substrates (for HRSEM investigations) kept at room temperature and rotated at a rate of 20 turn/min. During each turn pass the substrates spent over each crucible 0.25 sec; the time between the consecutive deposition of CdSe and ZnSe is 1.25 sec. Thus, small portions of ZnSe/CdSe were consecutively deposited at rates V_{dep} = 0.3 nm/sec (nominal thickness 0.075 nm), 0.5 nm/sec (nominal thickness 0.12 nm) and 0.9 nm/sec (nominal thickness 0.23 nm). The nominal thickness was determined by multiplying the deposition rate by the time substrates spent over the crucible. Both materials alloyed and form ternary $Zn_xCd_{1-x}Se$ films (Group I samples). The film composition was set by using appropriate deposition rate ($V_{dep}^{ZnSe}/V_{dep}^{CdSe}$: 0.3/0.9, 0.5/0.5, 0.9/0.3 nm/sec for films with x = 0.4, 0.6 and 0.8, respectively). For comparison Group II films of $Zn_xCd_{1-x}Se$ with the same thickness and composition were prepared at deposition rates of 0.5, 1.0 or 1.5 nm/sec [13, 14], as well as single layers of ZnSe and CdSe deposited on rotated substrates at the same substrate temperature. The deposition rates were controlled by two previously calibrated quartz microbalance systems MIKI FFV. A part of the Group I films were furnace annealed at T_a = 673 K for 60 min in an argon atmosphere.

Gracing Incidence XRD (GIXRD) experiments were performed on a X-ray Diffraction System (triple axis rotating anode) - *SmartLab* - 9kW rotating anode, in-plane arm (Rigaku Corporation, Japan) with Cu K_α radiation, $\lambda = 0.154$ nm. The GIXRD patterns realized at an angle of incidence $\alpha = 0.5^o$ were registered via the continuous method applying 0.01^o steps (2θ, θ is the Bragg angle) and a counting speed of 12.000 deg/min. The scattered X-ray radiation was detected with SC-70 detector. All XRD patterns were taken within an angular interval 2θ from 20° to 60° in which the main diffraction peaks of ZnSe and CdSe are located. High Resolution SEM images of the sample surfaces were obtained using a Nova NanoSEM 630 (FEI Company, USA) scanning electron microscope operating at an accelerating voltage of 10 kV. The grain size was estimated with SPIP^{tm} image processing software version 6.0.9 (Image metrology A/S).

RESULTS AND DISCUSSION

XRD spectra of ZnSe and CdSe single layers and three $Zn_xCd_{1-x}Se$ layers from Group I with x = 0.4, 0.6 and 0.8 are shown in Fig.1 (a). Similar series of spectra has been taken for the $Zn_xCd_{1-x}Se$ layers from Group II. A very intense diffraction peak is seen in all spectra which is centred in the range $2\theta = 25 - 27^o$. Its angular position is dependent on the film composition (x value). As expected, the decrease of the Zn content causes a shift of this peak to the higher angles in respect to its position in the spectrum of pure CdSe (for which x = 0). The reason for this is the larger atomic radius of Cd in comparison with the Zn atomic radius. The substitution of Cd with Zn atoms leads to decrease of the lattice parameter (i.e. to decrease of the interplanar spacing) and causes the observed shift of the diffraction peaks towards higher 2θ angles.

X-ray diffraction bands of much lower intensity were also detected. In order to analyze their behaviour the low-intense parts of the patterns are presented in an enlarged scale (Fig.1 (b)). Two additional peaks at $2\theta = 45.2^o$ and 53.5^o are revealed in the ZnSe spectrum while in the CdSe spectrum four additional peaks are observed at $2\theta \sim 35^o, 42^o, 46^o$ and 50° and also two low-intense bands at $2\theta \sim 24^o$ and 27° can be noticed. It is known, that both CdSe and ZnSe, can form cubic and hexagonal (wurtzite) polymorphous modifications. The three bands in the ZnSe

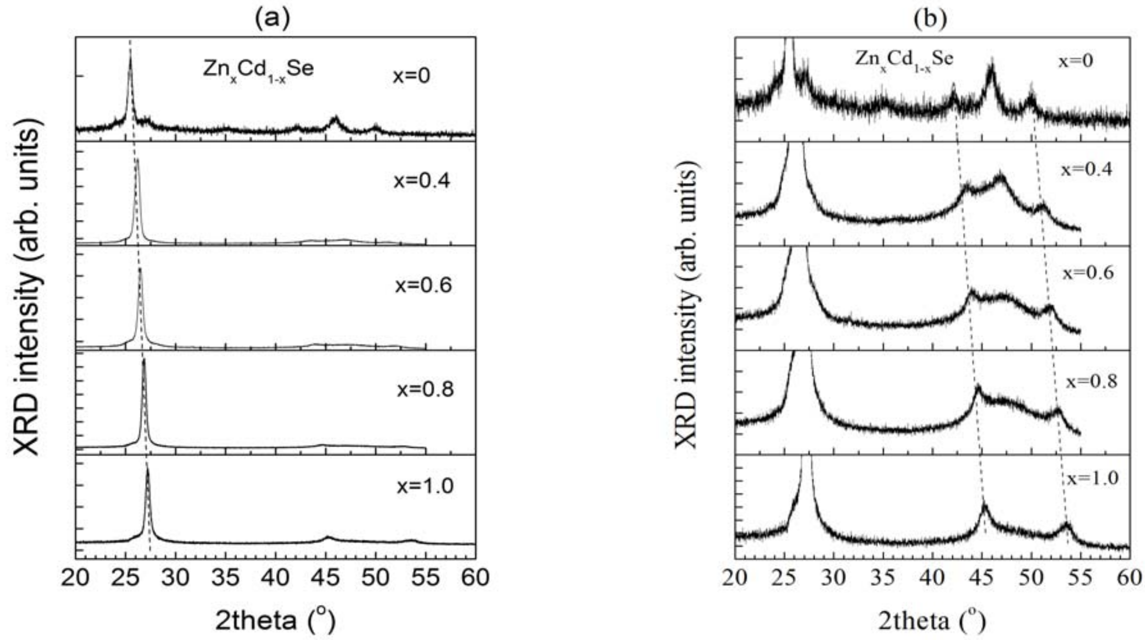

Fig. 1. (a) X-ray diffraction patterns of binary CdSe and ZnSe single layers and three $Zn_xCd_{1-x}Se$ layers from Group I; (b) a part of the patterns at an expanded y-scale. The dashed lines indicate the band shift to the higher angles when Zn content increases.

spectrum are typical for cubic ZnSe – the peaks at 27.225°, 45.196° and 53.569° are due to X-ray diffraction from the {111}, {220} and {311} families of crystallographic planes (JCPDS 05-0522). No bands appear that are characteristic for the wurtzite structure (JCPDS 15-0105), which indicates that at the preparation conditions applied the ZnSe films are entirely cubic. On the other hand the bands at 2θ ~ 24°, 27°, 35° and 46° are typical for wurtzite CdSe (diffraction from the {100} family of crystallographic planes at 23.97°, {101} at 27.1°, {102} at 35.1° and {103} at 45.8° (JCPDS 08-0459)). Since the intensity of these bands is rather low one can infer that here investigated CdSe single layer has predominantly cubic structure (JCPDS 19-0191) but small amount of wurtzite phase is also present. These results are in good agreement with the conclusions made in our previous studies on ZnSe [14] and CdSe [16] single layers which indicates a good reproducibility of the structure of the binary ZnSe and CdSe films. Similarly to the peak at 2θ ~ 27°, the two weak bands in the spectra of $Zn_xCd_{1-x}Se$ layers at ~ 43 - 44° and 51 - 52° are shifted towards higher angles as the Zn content increases (Fig.1 (b), dashed lines) but it is difficult to make a reliable conclusion for the shift of the middle band (at 2θ ~ 47°) since its intensity is rather low in the spectra of the films with greater Zn content. The intensity decrease of this band indicates that the wurtzite fraction in the ternary $Zn_xCd_{1-x}Se$ layers decreases with increasing Zn content though it is still noticeable in the x = 0.8 films.

Table 1. Angular position, full width at half maximum and integrated intensity of the strongest peak in the XRD spectra of as-deposited ZnxCd1-xSe thin films from Groups I and II.

$Zn_xCd_{1-x}Se$	XRD band center (deg)	FWHM (deg)	IiiiIntegrated Iintensity
x = 0.8, Group I			
as-deposited	26.85	0.41	21834
annealed	(1)26.79	0.34	10985
	(2)26.53	0.46	18369
x = 0.8, Group II			
as deposited	26.88	0.42	24308
x = 0.6, Group I			
as-deposited	26.49	0.49	14204
annealed	26.46	0.45	36198
x = 0.6, Group II			
as deposited	26.52	0.46	14080
x = 0.4, Group I			
as-deposited	26.18	0.52	21100
annealed	26.15	0.41	22552
x = 0.4, Group II			
as deposited	26.02	0.34	29200

In order to determine the position and FWHM of the strongest peak in the XRD spectra of Group I

and Group II as-deposited $Zn_xCd_{1-x}Se$ samples it was fitted with a single Lorentzian (only for the spectrum of Group I, annealed x = 0.8 film the fitting with two Lorentzians gave better result). The results obtained are summarized in Table 1. For the films with x = 0.6 and 0.8 both the positions and the FWHM are practically the same. For the films with x = 0.4 a small difference is observed in the peak positions and the FWHM of the film from the Group I is significantly larger than that of the Group II sample. These results indicate a good reproducibility of the film composition independently of the thickness of the ZnSe and CdSe sublayers.

For $Zn_xCd_{1-x}Se$ films prepared using the same way as that applied for the Group II film preparation we observed [14] some deviation of the lattice constant (calculated using the angular position of the {111} peak and assuming pure cubing structure) from the Vegard's rule for the films with $x \leq 0.6$. It has been assumed that this deviation is due to lattice distortion, which could be significant at the relatively high amount of Cd atoms. Based on the results of this study one can suggest that the observed deviation from the Vegard's rule is due to the appreciable amount of wurtzite phase in the films with relative high Cd content which may cause lattice distortion in the cubic phase.

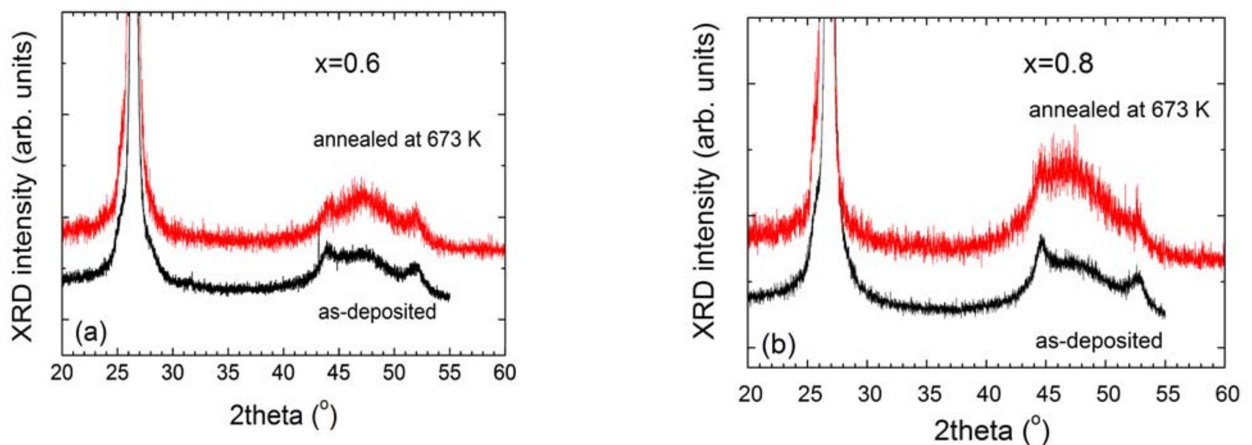

Fig. 2. X-ray diffraction patterns of as-deposited and annealed $Zn_xCd_{1-x}Se$ thin films from Group I with two compositions (x = 0.6 and x = 0.8) denoted in the figure.

X-ray diffraction patterns of as-deposited and annealed $Zn_xCd_{1-x}Se$ thin films from Group I with two compositions (x = 0.6 and 0.8) are depicted in Fig. 2. A comparison of the spectra shows that the film annealing at 673 K results in an intensity increase of the band at $2\theta \sim 47^o$ that is an indication that the amount of the wurtzite phase increases. Moreover, as seen from Table 1, the integrated intensity of the strongest band in the spectra of x = 0.4 and 0.6 annealed films increases but the peak position remains nearly the same as for the as-deposited films; in addition the FWHM is reduced. Only for the x = 0.8 sample an asymmetry is observed after annealing which has been discussed in more details in ref. 17. Annealing induced intensity increase has been also observed [15] for films deposited using the preparation conditions applied for the Group II samples. It is most likely related to an improvement of the film crystallinity and grain size increase. A small annealing induced shift of 0.07 - 0.1^o to higher Bragg angles was observed for the Group II type samples [15], which corresponds to a lattice constant decrease of ~ 0.02 nm. Therefore it has been ascribed to some annealing induced film densification. Should this be the case, the same position of the most intense band of the as-deposited and annealed films from Group I indicates that no annealing induced densification occurs and one can assume that these films are slightly denser than the films with thicker sublayers.

Let us now consider in more details the observed changes in the FWHM. As mentioned above the FWHM of the most intense band (at $2\theta \sim 27^o$) in the spectra of Group I as-deposited films is almost equal (x = 0.6 and 0.8) or higher (x = 0.4) than that of the Group II samples (Table 1). Moreover the annealing at 673 K causes FWHM

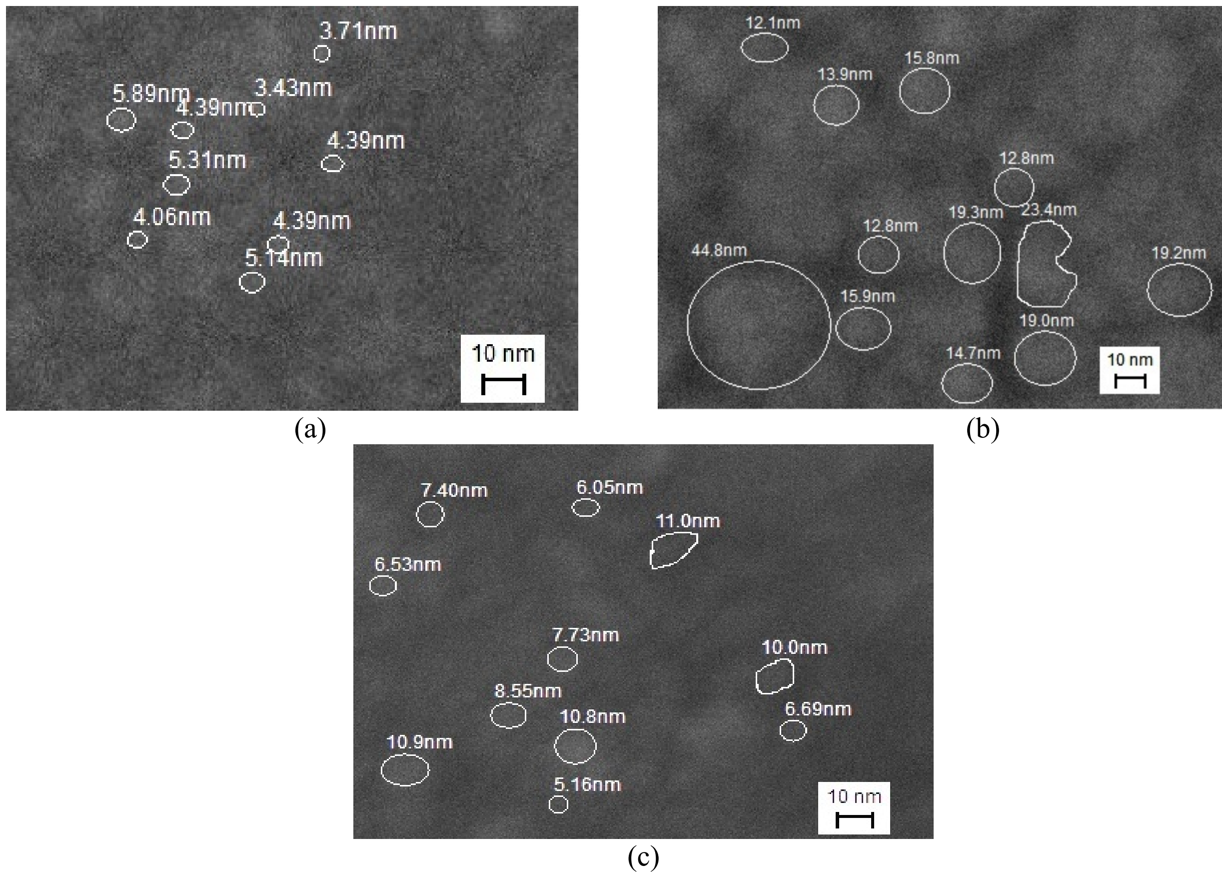

(a) (b)

(c)

Fig. 3. High resolution SEM surface images of: (a) as-deposited, (b) annealed Zn0.4Cd0.6Se films from Group I, (c) an as-deposited Zn0.4Cd0.6Se film from Group II. A part of the crystal grains are marked by white curves to make the size and shape clearer. The grain size values given in the figure were obtained by the SPIPtm image processing software.

decrease in the x = 0.4 films while for the other two compositions no appreciable decrease has been registered. It is known that both grain size and internal strain affect FWHM of the bands in XRD spectra of polycrystalline samples. The grain size decrease and the internal strain increase cause a FWHM increase. Hence the lower FWHM in the spectra of Group II as-deposited x = 0.4 film and the Group I annealed x = 0.4 film (Table 1) implies that the grain size in these films should be larger than that in the as-deposited Group I sample.

Information about the grain size has been obtained from the HRSEM investigation. HRSEM surface images of as-deposited and annealed x = 0.4 samples from Group I are shown in Fig.3 (a) and (b), respectively; HRSEM image of an as-deposited x = 0.4 sample from Group II is depicted in Fig. 3 (c). It is seen that most grains have close to spherical shape. For the Group I samples the grain size of the annealed film is larger than that of the as-deposited one. Moreover for the same composition of as-deposited films the grain size is larger in the Group II sample. The SPIP^{tm} image processing has given an average size of 4.6 nm in the Group I as-deposited film, while the size in the annealed film is approximately four times greater (17.4 nm); the size in the Group II as-deposited sample is about twice greater than that of the Group I sample (8.3 nm). These observations confirm the conclusion based on the XRD data. The HRSEM results for the other two compositions are similar to those obtained for x = 0.4 i.e. the grain size in as-deposited films of Group I is smaller than the size in the other two kinds of films. It is known [18] that in the films deposited by thermal evaporation in vacuum the grain size decreases with decreasing both film thickness and deposition rate (not too strongly in the latter case). Hence, the smallest grain size in the Group I as-deposited films can be related to both the lower sublayer thickness and the lower deposition rate used for the sample preparation.

No appreciable reduction of the FWHM values has been observed upon annealing of the x = 0.6 and 0.8 samples. Taking into account the strong annealing induced size increase which should cause

significant FWHM reduction, as well as the “27°” band intensity increase related to improved crystallinity, one can infer that in the annealed films with these compositions the internal strain is significantly higher than in the as-deposited ones. This strain increase could be related to some cracking observed in the SEM images of annealed samples [17].

CONCLUSIONS

Thin films of $Zn_xCd_{1-x}Se$ with x = 0.4, 0.6 and 0.8 were produced by alloying of consecutively deposited ultrathin, island type ZnSe and CdSe sublayers with various thicknesses. The influence of the sublayer thickness and furnace annealing on the crystallographic structure and microstructure of the films has been investigated. It has been shown that all $Zn_xCd_{1-x}Se$ films prepared have predominantly cubic structure independently of the sublayer thickness. A small amount of wurtzite phase has also been detected and it decreases with increasing Zn content. It has been suggested that the wurtzite phase in the Cd-enriched films causes some lattice distortion in the cubic phase which is the reason for the small lattice constant deviation from the Vegard’s rule reported earlier.

It has been found that in as-deposited films of each composition the grain size is influenced by the sublayer thickness; it is smaller in the films built of thinner sublayers. This observation has been related to the combined effect of the reduction of both sublayer thickness and deposition rate. It has also been concluded that the internal strain in the x = 0.6 and 0.8 annealed films is higher than in the as-deposited films.

Acknowledgements: *This work was supported by the Bulgarian Ministry of Education, Youth and Science under grant DMU 03-91.*

REFERENCES

1 R. Chandramohan, T. Mahalingam, J. P. Chu, P. J. Sebastian, *Sol. Energy Mater. Solar Cells,* **81**, 371 (2004).
2 S. Ham, S. Jeon, U. Lee, K.-J. Paeng, N. Myung, *Bull. Korean Chem. Soc.*, **29**, 939 (2008).
3 I. Suemune, T. Tawara, T. Saitoh, K. Uesugi, *Appl. Phys. Lett*., **71,** 3886 (1997).
4 M. C. H. Liao, Y. H. Chang, Y. F. Chen, J. W. Hsu, J. M. Lin, W. C. Chou, *Appl. Phys. Lett.,* **10,** 2256 (1997).
5 M. A. Hines, P. Guyot-Sionnest, *J. Phys. Chem. B,* **102,** 3655 (1998).
6 F. C. Peiris, S. Lee, U. Bindley, J. K. Furdina, *J. Appl. Phys*., **86,** 918 (1999).
7 O. Maksimov, W. H. Wang, N. Samarth, M. Munoz, M. C. Tamargo, *Solid State Commun*., **128**, 461 (2003).
8 L. Gupta, S. Rath, S. C. Abbi, F. C. Jain, *Pramana - journal of physics*, **61**, 729 (2003).
9 P. P. Hankare, P. A. Chate, M. R. Asabe, S. D. Delekar, I. S. Mulla, K. M. Garadkar, *J. Mater Sci: Mater Electronics*, **17**, 1055 (2006).
10 X. T. Zhang, Z. Liu, Li Quan, S. K. Hark, *J. Phys. Chem. B*, **109,** 17913 (2005).
11 D. S. Sutrave, G. S. Shahane, V. B. Patil, L. P. Deshmikh, *Turk J. Phys*., **24**, 63 (2000).
12 A. H. Ammar, *Vacuum*, **20**, 355 (2001).
13 D. Nesheva, Z. Aneva, M. J. Scepanovic, I. Bineva, Z. Levi, Z. V. Popovic, B. Pejova, *J. Phys.: Conf. Series*, **253**, 012035 (2010).
14 D. Nesheva, Z. Aneva, M. J. Scepanovic, Z. Levi, I. Iordanova, Z. V. Popovic, *J. Phys. D: Appl. Phys*., **44**, 415305 (2011).
15 I. Bineva, D. Nesheva, B. Pejova, M. Mineva, Z. Levi, Z. Aneva, *J. Phys.: Conf. Series*, **398**, 012015 (2012).
16 D. Nesheva, D. Arsova, R. Ionov, *J. Mater. Sci.,* **28**, 2183 (1993).
17 I. Bineva, A. Dinescu, D. Nesheva, M. Danila, Z. Aneva, Z. Levi, R. Muller, in IEEE Proc. Int. Semicond. Conf., CAS 2013, Bucharest, 2013, vol. 1, p.127.
18 K. L. Chopra, in Electrical phenomena in thin films, T. D. Shermergor (ed.), Mir, Moskva, 1972.

ВЛИЯНИЕ НА ДЕБЕЛИНАТА НА ПОДСЛОЕВЕТЕ И ОТГРЯВАНЕТО ВЪРХУ КРИСТАЛНАТА СТРУКТУРА И РАЗМЕРА НА ЗЪРНАТА НА НАНОКРИСТАЛНИ СЛОЕВЕ ОТ $Zn_XCd_{1-X}Se$

Д. Д. Нешева[1*], И. Е. Бинева[1], М. Данила[2], А. Динеску[2], З. М. Леви[1], З. И. Анева[1], Р. Мюлер[2]

[1]*Институт по физика на твърдото тяло, Българска академия на науките, бул. Цариградско шосе 72, 1784 София, България*
[2]*Национален институт за изследване и разработки в микротехнологиите - ИМТ Букурещ 126А, ул. Ероу Янку Николае, 077190 Букурещ, Румъния*

Постъпила на 17 октомври 2013 г.; коригирана на 25 ноември, 2013 г.

(Резюме)

С рентгенова дифракция и високо-разделителна сканираща електронна микроскопия (ВРСЕМ) е изследвано влиянието на дебелината на подслоевете и термично отгряване върху кристалографската структура и микроструктурата на 400 нм дебели слоеве от $Zn_xCd_{1-x}Se$ с $x = 0.4$, 0.6 и 0.8. Слоевете са изготвени с последователно отлагане на ултратънки слоеве от ZnSe и CdSe от островен тип с различна номинална дебелина (0.08, 0.12 и 0.23 нм). Направено е заключение, че всички слоеве са с доминиращо кубична структура, независимо от дебелината на подслоевете. Установено е и наличие на малко количество вюрцитна фаза, което намалява с увеличаване на съдържанието на Zn. От ВРСЕМ резултатите е направен извод, че за всеки състав на неотгретите слоеве размерът на кристалните зърна е по-малък в слоевете, изградени от по-тънки подслоеве. Вътрешните напрежения в отгретите слоеве с x=0.6 и 0.8 са по-големи от тези в неотгретите образци.